



TITLE:

Pathology of Idiopathic Pulmonary Fibrosis Assessed by a Combination of Microcomputed Tomography, Histology, and Immunohistochemistry

AUTHOR(S):

Tanabe, Naoya; McDonough, John E.; Vasilescu, Drago M.; Ikezoe, Kohei; Verleden, Stijn E.; Xu, Feng; Wuyts, Wim A.; Vanaudenaerde, Bart M.; Colby, Thomas V.; Hogg, James C.

CITATION:

Tanabe, Naoya ...[et al]. Pathology of Idiopathic Pulmonary Fibrosis Assessed by a Combination of Microcomputed Tomography, Histology, and Immunohistochemistry. *The American Journal of Pathology* 2020, 190(12): 2427-2435

ISSUE DATE:

2020-12

URL:

<http://hdl.handle.net/2433/259231>

RIGHT:

© 2020. This manuscript version is made available under the CC-BY-NC-ND 4.0 license <http://creativecommons.org/licenses/by-nc-nd/4.0/>; The full-text file will be made open to the public on 1 December 2021 in accordance with publisher's 'Terms and Conditions for Self-Archiving'; この論文は出版社版ではありません。引用の際には出版社版をご確認ご利用ください。 ; This is not the published version. Please cite only the published version.

1 **Pathology of idiopathic pulmonary fibrosis assessed by a combination of micro-computed**
2 **tomography, histology, and immunohistochemistry**

3

4 Naoya Tanabe^{1,2*}, John E. McDonough^{3,4*}, Dragoş M. Vasilescu^{1*}, Kohei Ikezoe^{1,2}, Stijn E.
5 Verleden⁴, Feng Xu¹, Wim A Wuyts⁴, Bart M. Vanaudenaerde⁴, Thomas V. Colby⁵, James C.
6 Hogg¹

7

8 ¹ Centre for Heart and Lung Innovation, at St. Paul's Hospital, University of British
9 Columbia, Vancouver, BC, Canada

10 ² Department of Respiratory Medicine, Graduate School of Medicine, Kyoto University,
11 Kyoto, Japan

12 ³ Department of Internal Medicine, Section of Pulmonary, Critical Care & Sleep Medicine,
13 Yale School of Medicine, New Haven, CT, USA

14 ⁴ KU Leuven, Department of Chronic disease, metabolism and aging, Laboratory of
15 Respiratory diseases, Leuven, Belgium

16 ⁵ Department of Laboratory Medicine and Pathology (Emeritus), Mayo Clinic, Scottsdale,
17 AZ, USA

18 * Authors contributed equally to this work.

19

20 **Number of text pages:** 23

21 **Number of tables:** 4

22 **Number of figures:** 3

23 **Short running head (40 characters or less):** Pathologist's scores and microCT in IPF

24 **Grant numbers and sources of support:** NT received the Dr. K. K. Pump Fellowship of the
25 BC Lung Association. DMV received a fellowship award from the Parker B. Francis

26 foundation. SEV is supported by a post doctoral fellowship of FWO (12G8718N) and a grant
27 from KU Leuven (C24/18/073)

28

29 **Disclosures:** Authors have no conflict of interest to declare.

30

31

32 **Corresponding author:**

33 Naoya Tanabe, MD, PhD

34 Centre for Heart and Lung Innovation, St. Paul's Hospital, University of British Columbia,

35 Vancouver, BC, Canada

36 166-1081 Burrard St, Vancouver, B.C., Canada, V6Z 1Y6

37 (Current address)

38 Department of Respiratory Medicine, Graduate School of Medicine, Kyoto University, Kyoto,

39 Japan

40 54 Kawahara-cho, Shogoin, Sakyo-ku, Kyoto 606-8507, Japan

41 Email: ntana@kuhp.kyoto-u.ac.jp

42

43

44 **Abstract (Unstructured, 218 /220 words)**

45 Idiopathic pulmonary fibrosis (IPF) is a fibrotic disease showing the histology of usual
46 interstitial pneumonia (UIP). While the pathologist's visual inspection is central in
47 histological assessments, three-dimensional microCT assessment may complement
48 pathologist's scoring. This study examined associations between the histopathological
49 features of UIP/IPF in explanted lungs and quantitative microCT measurements including
50 alveolar surface density, total lung volume taken up by tissue (tissue%), and terminal
51 bronchiolar number. Sixty frozen samples from 10 air-inflated explanted lungs with severe
52 IPF and 36 samples from 6 donor control lungs were scanned with microCT and processed for
53 histology. An experienced pathologist scored 3 major UIP criteria (patchy fibrosis,
54 honeycomb, and fibroblastic foci), 5 additional pathological changes such as emphysema, and
55 immunohistochemical staining for CD68, CD4, CD8, and CD79a positive cells, graded on a
56 0-3+ scale. The alveolar surface density and terminal bronchiolar number decreased and the
57 tissue% increased in IPF compared to controls. In lungs with IPF, lower alveolar surface
58 density and higher tissue% were correlated with greater scores of patchy fibrosis, fibroblastic
59 foci, honeycomb, CD79a-positive cells, and lymphoid follicles. A decreased number of
60 terminal bronchioles was correlated with honeycomb score, but not with the other scores. The
61 three-dimensional microCT measurements reflect the pathological UIP/IPF criteria and
62 further suggest that the reduction in the terminal bronchioles may be associated with
63 honeycomb cyst formation.

64

65

66 **Keywords:** MicroCT, Interstitial lung disease, lung, airway, pulmonary fibrosis

67

68

69

70 **List of abbreviation:**

71 IPF = Idiopathic pulmonary fibrosis

72 Lm = Mean linear intercept

73 Tissue% = total lung volume taken up by tissue

74 UIP = Usual interstitial pneumonia

75

76

77 This paper includes an online supplemental video.

78

79 Introduction

80 Idiopathic pulmonary fibrosis (IPF) is a chronic fibrotic disease characterized by a
81 rapid decline in lung function and poor prognosis¹. The ATS/JRS/and Latin American (ALAT)
82 guidelines all recommended for the diagnosis and management² based on an integrative
83 multidisciplinary assessment of clinical information, radiological assessment, histopathologic
84 diagnosis, but while diagnosis can be confirmed without histology in cases that present
85 features of IPF including honeycomb cysts on high resolution computed tomography
86 (HRCT)², histological assessment remains important especially for diagnosing the early stage
87 of IPF and also for improving understanding of the pathogenesis of the disease.

88 The histopathological changes in IPF are characterized by patchy dense fibrosis that is
89 often accompanied by honeycomb cyst formation². Proliferating fibroblasts and
90 myofibroblasts produce collagen in the active regions of fibroplasia, termed fibroblastic foci³⁻
91 ⁵. In contrast, the infiltration of inflammatory immune cells into fibrotic regions is generally
92 considered to be mild². However, recent histology and gene expression analyses have
93 suggested that a B cell-mediated immune response and lymphoid follicles formations may be
94 associated with fibrosis⁶⁻⁹.

95 The pathologist's visual scoring of UIP/IPF features on lung samples from surgical
96 lung biopsy is essential in histological assessment^{1,2}. Although the morphometric approach
97 has been less used in the examination of IPF lungs compared to other lung diseases such as
98 COPD¹⁰⁻¹³, studies have suggested that alveolar collapse onto the alveolar duct mainly
99 contributes to a reduction in alveolar surface area and impairs diffusion capacity in patients
100 with IPF¹⁴⁻¹⁶. Nonetheless, little remains known regarding direct associations between
101 histologic features of UIP/IPF and quantitative morphometric indices, including the mean
102 linear intercept (Lm), total lung volume taken up by tissue (tissue%), alveolar surface density
103 defined as alveolar surface area per lung volume¹⁷.

104 The introduction of micro-computed tomography (microCT) has enabled three-
105 dimensional (3D) morphological assessments of lung tissues that are very difficult to achieve
106 with conventional histology^{12, 13, 18, 19}. In addition, microCT scans of frozen air-inflated tissue
107 enable quantitative assessment without shrinkage and physical cutting of tissues²⁰. Mai et al.¹⁶
108 combined CT, microCT, and histological assessments, and showed that fibrosis and
109 honeycomb cysts formation in IPF extends from the peripheral to the central region of the
110 pulmonary lobules. Further, McDonough et al.²¹ presented preliminary microCT based
111 analysis of the complex relationship between honeycomb cysts and conducting airways at the
112 American Thoracic Society International Conference which suggested that the honeycomb
113 cyst formation could be a result of airway remodeling. Very recently, Verleden et al.²²
114 proposed the importance of the small airway disease in IPF by showing that the numbers of
115 the terminal bronchioles (defined as the last generation of the conducting airways) were
116 reduced in lungs with end stage IPF compared to control lungs. Collectively, these findings
117 have demonstrated that quantitative morphometric microCT measurements complement the
118 pathologist's visual inspections of lungs with IPF.

119 The aim of this study was to extend the understanding of the pathology of UIP/IPF
120 lungs by investigating the relationship between the experienced pathologist's scorings of
121 histological features such as honeycomb cysts and microCT measurements of alveolar surface
122 density, tissue%, Lm, and the number of the terminal bronchioles.

123

124 **Materials and Methods**

125 **Informed consent:** was obtained either directly from the patient or from the next of kin of the
126 donors that served as controls under conditions approved by the ethical (S52174) and biosafety
127 (MS20101571) committees at the Katholieke Universiteit Leuven and accepted by all the other
128 participating institutions.

129 **Protocol:** A diagnosis of IPF was based on the current ATS/ERS/JRS/ATLT guidelines that
130 include dominant airway-centered changes as an exclusion criterion^{1, 2}. The major features of
131 this protocol have been described in detail elsewhere^{9, 22, 23}. Briefly intact lung specimens
132 donated by patients with very severe IPF treated by lung transplantation and unused donor lungs
133 that served as controls were inflated with air and frozen solid with liquid nitrogen vapor. The
134 specimen was kept frozen while cutting it into 2 cm thick transverse slices. Two lung tissue
135 samples were obtained from either the upper, middle, and lower part of the lung (n=6 per lung)
136 to compare samples with different severity of the disease^{9, 22, 23}.

137 **MicroCT-based morphometric quantification:** The tissue samples were kept frozen while
138 scanned at 9.98 μm voxel resolution with a SkyScan 1172 scanner (Kontich, Belgium)²². As
139 previously described, image thresholding was applied to separate tissue and airspaces. The
140 tissue segmentation was used to compute tissue% and alveolar surface density (defined as
141 alveolar surface area per volume of lung^{9, 23}). The airspace segmentation was used to compute
142 the mean airspace size (mean linear intercept, Lm) by measuring and averaging interalveolar
143 wall distances²². The terminal bronchioles were defined as the last generation of conducting
144 bronchioles and counted manually in the microCT scans of each sample. The number of
145 terminal bronchioles per ml of lung was calculated by dividing the number per sample by the
146 sample volume^{13, 20}.

147 **Histology:** The pathologist's scoring was performed in the present study using histological
148 sections obtained in the previous IPF study²². Following microCT imaging, portions of the
149 frozen samples were fixed in alcohol-based formalin at -20°C overnight, warmed to room
150 temperature, and then processed into paraffin blocks from which histological sections were cut
151 and stained with H&E and Movat Pentachrome stains. As shown in Figure 1, these histological
152 sections were examined by an experienced pulmonary pathologist (TVC) who scored 8
153 pathological features that consisted of the 3 major UIP criteria including patchy fibrosis,

154 honeycomb cyst formation, and fibroblastic foci, as well as 5 additional pathological changes
155 including emphysema, degree of inflammation, hyaline membrane formation, lymphoid
156 follicles, and respiratory bronchiolitis, all on a 0-3+ scale. In addition, other portions of the
157 frozen samples were briefly warmed to -1°C , vacuum embedded in the optimum cutting
158 temperature compound (OCT, SAKURA FINETEK), immediately returned to -80°C , and cut
159 into serial frozen sections ($8\ \mu\text{m}$ thick) for immunohistochemistry. These sections were stained
160 with primary antibodies for CD68 (DAKO, M0876, 1:200 dilution), CD4 (DAKO, M7310,
161 1:200 dilution), CD8 (DAKO, M7103, 1:400 dilution), and CD79a (DAKO, M7050, 1:200
162 dilution) as previously reported²². These sections were also scored by the same pathologist on
163 a 0-3+ scale.

164 **Statistical Analysis:** Data are expressed as mean \pm standard deviation. Statistical analysis was
165 performed with the R statistical program (R Core Team: R: A Language and Environment for
166 Statistical Computing. URL <http://www.R-project.org/>. accessed 2019 Nov 1. version 3.4.1).
167 The Spearman correlation tests and Mann Whitney comparison were used for correlation tests
168 and group comparisons, respectively. Multiple comparisons were performed with Wilcoxon
169 tests with Holm correction.

170

171 **Results**

172 Table 1 shows that there is no difference in age, sex, height, or weight between the
173 patients with IPF and the control subjects. Table 2 summarizes microCT and histological scores.
174 Alveolar surface density and the number of terminal bronchioles /ml lung were lower, while
175 tissue% and Lm were higher in IPF compared to controls. In addition, CD68, CD4, CD8, and
176 CD79a positive cells were greater in IPF than controls. Supplemental figure 1 demonstrates that
177 the significant difference between IPF and controls was also present when comparing microCT
178 indices in the upper, middle, and lower regions separately.

179 Figure 2A and B show examples of histological regions with and without honeycomb
 180 formation (score 0 and 1, respectively) that were registered to the microCT scans. Figure 2C
 181 and D show that the alveolar surface density and number of terminal bronchioles were lower in
 182 the honeycomb regions (Score \geq 1) than in the non-honeycomb regions (Score=0). This finding
 183 was visualized on Figure 2E and a video that shows a microCT stack of the same sample as
 184 used in Figure 2B and E (Supplemental video 1). The video shows that many branches of the
 185 small airway tree (pink) were located in the “normal” appearing regions, but not in the
 186 honeycomb region, and that the conducting airway leading into the honeycomb region was
 187 directly connected to those severely distorted airspaces (orange). Further, Figure 3 shows that
 188 the decreases in the alveolar surface density and number of terminal bronchioles in the
 189 honeycomb region were also confirmed in a subanalysis that included non-emphysematous IPF
 190 samples (histological emphysema score =0) and controls.

191 Table 3 shows Spearman correlation coefficients between microCT indices and
 192 pathological scores in IPF samples (n=59). Decreased alveolar surface density and increased
 193 tissue% and Lm on microCT were correlated with the histological scores of patchy fibrosis,
 194 fibroblastic foci, and honeycomb. In contrast, decreased number of the terminal bronchioles
 195 was correlated with an increased score of honeycomb, but not with patchy fibrosis and
 196 fibroblastic foci.

197 Table 4 shows Spearman correlation coefficients between microCT indices and scores
 198 of lymphoid cells in IPF samples (n=60). Increased tissue% was correlated with increased
 199 scores for CD68, CD4, CD8, and CD79a positive cells and lymphoid follicles, whereas Lm and
 200 the number of terminal bronchioles were not associated with any of the scores of immune cells
 201 and lymphoid follicles.

202

203 **Discussion**

204 This study compared standard histopathological criteria of UIP/IPF and quantitative
205 morphological measures obtained from microCT. The microCT findings of decreased alveolar
206 surface density and increased tissue% were positively associated with the pathologist's
207 scoring of patchy fibrosis, fibroblastic foci, honeycomb formation, infiltration of CD79a-
208 positive lymphocytes, and lymphoid follicle formation. Furthermore, a combination of
209 histological assessment and the three-dimensional microCT information revealed that a
210 reduction in the number of terminal bronchioles was associated with honeycomb formation,
211 but not with patchy fibrosis or fibroblastic foci. These findings indicate that three-dimensional
212 morphometric assessment via microCT can be used to complement the pathologist's visual
213 inspection to by showing the pathological relationship between the peripheral airways and
214 parenchyma in lungs with IPF.

215 From a histopathological perspective, UIP/IPF lungs are characterized by spatially
216 heterogeneous fibrosis with fibroblastic foci and honeycomb lesion¹⁻³, and from a
217 physiological perspective, IPF lungs are characterized by impaired diffusion capacity which
218 affects the mortality²⁴. This structure-function relationship has been explained by multiple
219 morphometric studies showing that a collapse of alveoli onto the alveolar ducts in IPF lung
220 leads to a reduction of alveolar surface area^{14, 15, 25}. However, to the best of knowledge, no
221 prior report has tested the direct relationship between the pathological UIP/IPF criteria and
222 morphometric assessment of IPF lung. Therefore, the close correlations between alveolar
223 surface density, tissue%, and the histopathological scores of UIP/IPF presented here provide
224 an explanation for the clinically relevant impairment in diffusion capacity present in IPF
225 patients.

226 The widely accepted hypothesis that IPF is generally a parenchymal disease in which
227 the airways are spared was recently challenged by a microCT-based study that showed a loss
228 of the terminal bronchiole number already occurs in minimal fibrotic regions in lungs with

229 IPF compared to controls²². Since the terminal bronchioles are located in the centre of the
230 secondary lobules, these recent microCT findings have raised the question if there is an
231 interaction between small airway disease, such as loss of the terminal bronchioles, and
232 parenchymal pathology, such as alveolar collapse. The present study sheds light on this issue
233 by showing that the loss of terminal bronchioles is associated with honeycomb formation, but
234 not with patchy fibrosis, which leads to the conclusion that these might be two somewhat
235 separate process. This finding is consistent with the hypothesis proposed by Evans et al.²⁶ that
236 the peripheral airway injury is associated with honeycomb cyst formation independent of
237 fibroproliferation in the parenchyma. In addition, although COPD studies have shown a close
238 association between emphysema and a reduction in the terminal bronchioles^{13, 27, 28}, the
239 reduced number of terminal bronchioles in the honeycomb regions was confirmed even in the
240 subanalysis that excluded IPF samples with emphysema (histological score ≥ 1).

241 Furthermore, the supplemental video 1 provided portrays the 3D spatial relationship
242 between the small conducting airways and microscopic honeycomb regions, which on the
243 conventional 2D histological sections would be difficult to detect. The 3D visualization
244 demonstrates that the conducting airways are directly connected to the air spaces within the
245 honeycomb regions. This finding suggests that the potential airways present within the
246 honeycomb region are remodeled beyond recognition, and the small airways might be an
247 origin of honeycomb cysts in IPF. This concept requires further detailed investigation which
248 is beyond the scope of the present study.

249 Staats et al.²⁹ showed that a histologic finding of bronchiolectasis is associated with
250 honeycomb score on high-resolution CT (HRCT), and Walsh et al.³⁰ showed that traction
251 bronchiectasis on HRCT is closely associated with fibroblastic foci profusion on histology.
252 These suggest that traction bronchiectasis and honeycombing are part of a “continuous
253 spectrum of lung remodeling” as noted in clinical observations³¹, and are in line with the

254 present microCT findings that demonstrate a direct communication between the small airway
255 tree and honeycomb regions in lungs with IPF.

256 Together with previous findings that the polymorphism in the promoter region of the
257 MUC5B gene which regulates mucin production from bronchiolar epithelium is associated
258 with the pathogenesis of IPF^{26, 32} and the honeycomb regions are lined with bronchiolar-like
259 epithelium³³, we speculate that the terminal bronchiole remodeling might be involved in the
260 honeycomb formation.

261 This study used a single histological section for each tissue sample. Although
262 microscopic pathologies could vary throughout the tissue sample, it is speculated that within-
263 sample variation is smaller than the inter-samples variation because the cylindrical tissue
264 samples used in this study are relatively small (20 mm high and 14 mm in diameter).
265 Moreover, the close correlation between the pathologist's score of patchy fibrosis and the
266 tissue % on microCT that was obtained from the entire microCT stack, suggests that the single
267 histological section is sufficiently representative of the pathology of the sample core.

268 Extensive research has shown that a transition of fibroblasts into synthetic
269 myofibroblast, and subsequent deposition of collagen, plays an important role in the
270 progressive fibrotic process after repeated injuries in IPF^{34, 35}, however, the role of
271 inflammatory immune cells is not established. Histological studies have found infiltration of
272 inflammatory immune cells such as B cell aggregates^{8, 36, 37} while clinical trials using
273 immunosuppressive therapy have consistently failed to show the effectiveness in patients with
274 IPF³⁸. A recent study by Verleden et al. showed that the CD79a positive cell infiltration and
275 lymphoid follicle formation are present even in minimal fibrotic regions of IPF lungs²². The
276 present finding extends it by demonstrating an association of lymphoid follicle formation
277 score with increased tissue% and decreased alveolar surface density and further supports the

278 notion that the persistent adaptive immune response contributes to a fibrotic remodeling
279 process in IPF.

280 Moreover, an increase in CD68-positive cells was associated with the increased
281 tissue% in IPF lungs. This finding is consistent with the hypothesis that macrophages are
282 mainly involved in the pathogenesis of IPF^{39, 40} but could also in part reflect the smoking
283 history in all the patients. Macrophages are subcategorized into functional phenotypes such as
284 M1 and M2, and play various roles in the lung, including host defense to external insults and
285 wound healing after injury⁴¹. Therefore, in addition to staining with CD68 antibody, different
286 approach such as gene expression profiling and flowcytometry should be integrated in a future
287 study to explore the pathogenic roles of each macrophage phenotype in IPF.

288 There are limitations in the present study worth noting. First, all cases with IPF were
289 from former smokers. Since smoking is a major cause of emphysema that is closely associated
290 with the loss of the terminal bronchioles^{13, 27, 28}, the present finding of reduced number of
291 terminal bronchioles in IPF might have been affected by smoking. However, there was no
292 correlation between the pathologist's score for emphysema and the number of terminal
293 bronchioles, suggesting that the influence of smoking-related emphysematous destruction is
294 minimal in this study. Second, the sample number is small and all cases were very-severe IPF
295 that required lung transplantation. In order to broaden insights into disease phenotypes, it
296 would be beneficial if the design of future studies would include lung specimen from subjects
297 with different stages of IPF as well as different smoking status (i.e. both smokers and non-
298 smokers). Third, the static cross-sectional nature of the study limits causal inferences.
299 Therefore, the present study was not able to test whether patchy fibrosis and honeycomb cysts
300 formation induce infiltration of immune cells in IPF lungs or if specific immune cells induce a
301 fibrotic process in IPF lungs.

302 In conclusion, this is the first study to show that quantitative morphometric microCT
303 measurements of alveolar surface density, tissue%, and Lm are closely associated with the
304 general histo-pathological scoring of patchy fibrosis, fibroblastic foci and honeycomb lesions
305 in IPF. These data suggest that microCT measurements provide a reliable structural
306 assessment of IPF lungs especially since the established major criteria of UIP/IPF are
307 associated with reduced alveolar surface area which potentially impairs diffusion capacity in
308 IPF patients. Furthermore, the three-dimensional microCT evaluation revealed that
309 honeycomb formation, but not patchy fibrosis, is associated with a greater reduction in the
310 number of terminal bronchioles in IPF. Volumetric microCT based quantification of the lung
311 structure complements histological assessment of cellular composition of IPF lungs, and by
312 combining these methods with subsequent gene expression analysis or single cell sequencing
313 it may be possible to identify a novel therapeutic target for this devastating lung disease.

314

315 **Acknowledgments:** The authors would like to thank Fanny Chu and Jingwen Pan with their
316 assistance in histological preparation and staining, both from the Centre for Heart Lung
317 Innovation, University of British Columbia.

318

319

320 **References**

- 321 [1] Raghu G, Collard HR, Egan JJ, Martinez FJ, Behr J, Brown KK, Colby TV, Cordier JF,
322 Flaherty KR, Lasky JA, Lynch DA, Ryu JH, Swigris JJ, Wells AU, Ancochea J, Bouros D,
323 Carvalho C, Costabel U, Ebina M, Hansell DM, Johkoh T, Kim DS, King TE, Jr., Kondoh Y,
324 Myers J, Muller NL, Nicholson AG, Richeldi L, Selman M, Dudden RF, Griss BS, Protzko SL,
325 Schunemann HJ, Fibrosis AEJACoIP: An official ATS/ERS/JRS/ALAT statement: idiopathic
326 pulmonary fibrosis: evidence-based guidelines for diagnosis and management. *Am J Respir Crit*
327 *Care Med* 2011, 183:788-824.
- 328 [2] Raghu G, Remy-Jardin M, Myers JL, Richeldi L, Ryerson CJ, Lederer DJ, Behr J, Cottin V,
329 Danoff SK, Morell F, Flaherty KR, Wells A, Martinez FJ, Azuma A, Bice TJ, Bouros D, Brown
330 KK, Collard HR, Duggal A, Galvin L, Inoue Y, Jenkins RG, Johkoh T, Kazerooni EA, Kitaichi
331 M, Knight SL, Mansour G, Nicholson AG, Pipavath SNJ, Buendia-Roldan I, Selman M, Travis
332 WD, Walsh S, Wilson KC, American Thoracic Society ERSJRS, Latin American Thoracic S:
333 Diagnosis of Idiopathic Pulmonary Fibrosis. An Official ATS/ERS/JRS/ALAT Clinical
334 Practice Guideline. *Am J Respir Crit Care Med* 2018, 198:e44-e68.
- 335 [3] Katzenstein AL, Mukhopadhyay S, Myers JL: Diagnosis of usual interstitial pneumonia and
336 distinction from other fibrosing interstitial lung diseases. *Hum Pathol* 2008, 39:1275-94.
- 337 [4] Cool CD, Groshong SD, Rai PR, Henson PM, Stewart JS, Brown KK: Fibroblast foci are
338 not discrete sites of lung injury or repair: the fibroblast reticulum. *Am J Respir Crit Care Med*
339 2006, 174:654-8.
- 340 [5] King TE, Jr., Schwarz MI, Brown K, Tooze JA, Colby TV, Waldron JA, Jr., Flint A,
341 Thurlbeck W, Cherniack RM: Idiopathic pulmonary fibrosis: relationship between
342 histopathologic features and mortality. *Am J Respir Crit Care Med* 2001, 164:1025-32.

- 343 [6] Bringardner BD, Baran CP, Eubank TD, Marsh CB: The role of inflammation in the
344 pathogenesis of idiopathic pulmonary fibrosis. *Antioxid Redox Signal* 2008, 10:287-301.
- 345 [7] DePianto DJ, Chandriani S, Abbas AR, Jia G, N'Diaye EN, Caplazi P, Kauder SE, Biswas
346 S, Karnik SK, Ha C, Modrusan Z, Matthay MA, Kukreja J, Collard HR, Egen JG, Wolters PJ,
347 Arron JR: Heterogeneous gene expression signatures correspond to distinct lung pathologies
348 and biomarkers of disease severity in idiopathic pulmonary fibrosis. *Thorax* 2015, 70:48-56.
- 349 [8] Xue J, Kass DJ, Bon J, Vuga L, Tan J, Csizmadia E, Otterbein L, Soejima M, Levesque MC,
350 Gibson KF, Kaminski N, Pilewski JM, Donahoe M, Scirba FC, Duncan SR: Plasma B
351 lymphocyte stimulator and B cell differentiation in idiopathic pulmonary fibrosis patients. *J*
352 *Immunol* 2013, 191:2089-95.
- 353 [9] McDonough JE, Kaminski N, Thienpont B, Hogg JC, Vanaudenaerde BM, Wuyts WA:
354 Gene correlation network analysis to identify regulatory factors in idiopathic pulmonary fibrosis.
355 *Thorax* 2018.
- 356 [10] Tanabe N, Vasilescu DM, Hague CJ, Ikezoe K, Murphy DT, Kirby M, Stevenson CS,
357 Verleden SE, Vanaudenaerde BM, Gayan-Ramirez G, Janssens W, Coxson HO, Pare PD, Hogg
358 JC: Pathological Comparisons of Paraseptal and Centrilobular Emphysema in COPD. *Am J*
359 *Respir Crit Care Med* 2020.
- 360 [11] Vasilescu DM, Martinez FJ, Marchetti N, Galban CJ, Hatt C, Meldrum CA, Dass C,
361 Tanabe N, Reddy RM, Lagstein A, Ross BD, Labaki WW, Murray S, Meng X, Curtis JL,
362 Hackett TL, Kazerooni EA, Criner GJ, Hogg JC, Han MK: Noninvasive Imaging Biomarker
363 Identifies Small Airway Damage in Severe Chronic Obstructive Pulmonary Disease. *Am J*
364 *Respir Crit Care Med* 2019, 200:575-81.
- 365 [12] Tanabe N, Vasilescu DM, McDonough JE, Kinose D, Suzuki M, Cooper JD, Pare PD,
366 Hogg JC: Micro-Computed Tomography Comparison of Preterminal Bronchioles in
367 Centrilobular and Panlobular Emphysema. *Am J Respir Crit Care Med* 2017, 195:630-8.

- 368 [13] McDonough JE, Yuan R, Suzuki M, Seyednejad N, Elliott WM, Sanchez PG, Wright AC,
369 Gefter WB, Litzky L, Coxson HO, Pare PD, Sin DD, Pierce RA, Woods JC, McWilliams AM,
370 Mayo JR, Lam SC, Cooper JD, Hogg JC: Small-airway obstruction and emphysema in chronic
371 obstructive pulmonary disease. *N Engl J Med* 2011, 365:1567-75.
- 372 [14] Coxson HO, Hogg JC, Mayo JR, Behzad H, Whittall KP, Schwartz DA, Hartley PG, Galvin
373 JR, Wilson JS, Hunninghake GW: Quantification of idiopathic pulmonary fibrosis using
374 computed tomography and histology. *Am J Respir Crit Care Med* 1997, 155:1649-56.
- 375 [15] Lutz D, Gazdhar A, Lopez-Rodriguez E, Ruppert C, Mahavadi P, Gunther A, Klepetko W,
376 Bates JH, Smith B, Geiser T, Ochs M, Knudsen L: Alveolar derecruitment and collapse
377 induration as crucial mechanisms in lung injury and fibrosis. *Am J Respir Cell Mol Biol* 2015,
378 52:232-43.
- 379 [16] Mai C, Verleden SE, McDonough JE, Willems S, De Wever W, Coolen J, Dubbeldam A,
380 Van Raemdonck DE, Verbeken EK, Verleden GM, Hogg JC, Vanaudenaerde BM, Wuyts WA,
381 Verschakelen JA: Thin-Section CT Features of Idiopathic Pulmonary Fibrosis Correlated with
382 Micro-CT and Histologic Analysis. *Radiology* 2016:152362.
- 383 [17] Hsia CC, Hyde DM, Ochs M, Weibel ER, Structure AEJTFoQAoL: An official research
384 policy statement of the American Thoracic Society/European Respiratory Society: standards
385 for quantitative assessment of lung structure. *Am J Respir Crit Care Med* 2010, 181:394-418.
- 386 [18] Verleden SE, Vanstapel A, De Sadeleer L, Weynand B, Boone M, Verbeken E, Piloni D,
387 Van Raemdonck D, Ackermann M, Jonigk DD, Verschakelen J, Wuyts WA: Quantitative
388 analysis of airway obstruction in lymphangiomyomatosis. *Eur Respir J* 2020, 56.
- 389 [19] Bourdin A, Gamez AS, Vachier I, Crestani B: LAM is another small airway disease:
390 lessons from microCT. *Eur Respir J* 2020, 56.
- 391 [20] Vasilescu DM, Phillion AB, Tanabe N, Kinose D, Paige DF, Kantrowitz JJ, Liu G, Liu H,
392 Fishbane N, Verleden SE, Vanaudenaerde BM, Lenburg ME, Stevenson CS, Spira A, Cooper

- 393 JD, Hackett TL, Hogg JC: Non-destructive cryo micro CT imaging enables structural and
394 molecular analysis of human lung tissue. *J Appl Physiol* (1985) 2016:jap 00838 2016.
- 395 [21] McDonough JE, Verleden SE, Verschakelen J, Wuyts W, Vanaudenaerde BM: The
396 Structural Origin of Honeycomb Cysts in IPF. *D28 RESPIRATORY DISEASE DIAGNOSIS:
397 PULMONARY FUNCTION TESTING AND IMAGING: American Thoracic Society, 2018.*
398 pp. A6388-A.
- 399 [22] Verleden SE, Tanabe N, McDonough JE, Vasilescu DM, Xu F, Wuyts WA, Piloni D, De
400 Sadeleer L, Willems S, Mai C, Hostens J, Cooper JD, Verbeken EK, Verschakelen J, Galban
401 CJ, Van Raemdonck DE, Colby TV, Decramer M, Verleden GM, Kaminski N, Hackett TL,
402 Vanaudenaerde BM, Hogg JC: Small airways pathology in idiopathic pulmonary fibrosis: a
403 retrospective cohort study. *Lancet Respir Med* 2020, 8:573-84.
- 404 [23] McDonough JE, Ahangari F, Li Q, Jain S, Verleden SE, Herazo-Maya J, Vukmirovic M,
405 DeIuliis G, Tzouvelekis A, Tanabe N, Chu F, Yan X, Verschakelen J, Homer RJ, Manatakis
406 DV, Zhang J, Ding J, Maes K, De Sadeleer L, Vos R, Neyrinck A, Benos PV, Bar-Joseph Z,
407 Tantin D, Hogg JC, Vanaudenaerde BM, Wuyts WA, Kaminski N: Transcriptional regulatory
408 model of fibrosis progression in the human lung. *JCI Insight* 2019, 4.
- 409 [24] King TE, Jr., Tooze JA, Schwarz MI, Brown KR, Cherniack RM: Predicting survival in
410 idiopathic pulmonary fibrosis: scoring system and survival model. *Am J Respir Crit Care Med*
411 2001, 164:1171-81.
- 412 [25] Myers JL, Katzenstein AL: Epithelial necrosis and alveolar collapse in the pathogenesis of
413 usual interstitial pneumonia. *Chest* 1988, 94:1309-11.
- 414 [26] Evans CM, Fingerlin TE, Schwarz MI, Lynch D, Kurche J, Warg L, Yang IV, Schwartz
415 DA: Idiopathic Pulmonary Fibrosis: A Genetic Disease That Involves Mucociliary Dysfunction
416 of the Peripheral Airways. *Physiol Rev* 2016, 96:1567-91.

- 417 [27] Koo HK, Vasilescu DM, Booth S, Hsieh A, Katsamenis OL, Fishbane N, Elliott WM,
418 Kirby M, Lackie P, Sinclair I, Warner JA, Cooper JD, Coxson HO, Pare PD, Hogg JC, Hackett
419 TL: Small airways disease in mild and moderate chronic obstructive pulmonary disease: a cross-
420 sectional study. *Lancet Respir Med* 2018, 6:591-602.
- 421 [28] Tanabe N, Vasilescu DM, Kirby M, Coxson HO, Verleden SE, Vanaudenaerde BM,
422 Kinose D, Nakano Y, Pare PD, Hogg JC: Analysis of airway pathology in COPD using a
423 combination of computed tomography, micro-computed tomography and histology. *Eur Respir*
424 *J* 2018, 51.
- 425 [29] Staats P, Kligerman S, Todd N, Tavora F, Xu L, Burke A: A comparative study of
426 honeycombing on high resolution computed tomography with histologic lung remodeling in
427 explants with usual interstitial pneumonia. *Pathol Res Pract* 2015, 211:55-61.
- 428 [30] Walsh SL, Wells AU, Sverzellati N, Devaraj A, von der Thusen J, Yousem SA, Colby TV,
429 Nicholson AG, Hansell DM: Relationship between fibroblastic foci profusion and high
430 resolution CT morphology in fibrotic lung disease. *BMC Med* 2015, 13:241.
- 431 [31] Piciucchi S, Tomassetti S, Ravaglia C, Gurioli C, Gurioli C, Dubini A, Carloni A, Chilosi
432 M, Colby TV, Poletti V: From "traction bronchiectasis" to honeycombing in idiopathic
433 pulmonary fibrosis: A spectrum of bronchiolar remodeling also in radiology? *BMC Pulm Med*
434 2016, 16:87.
- 435 [32] Hunninghake GM, Hatabu H, Okajima Y, Gao W, Dupuis J, Latourelle JC, Nishino M,
436 Araki T, Zazueta OE, Kurugol S, Ross JC, San Jose Estepar R, Murphy E, Steele MP, Loyd JE,
437 Schwarz MI, Fingerlin TE, Rosas IO, Washko GR, O'Connor GT, Schwartz DA: MUC5B
438 promoter polymorphism and interstitial lung abnormalities. *N Engl J Med* 2013, 368:2192-200.
- 439 [33] Seibold MA, Smith RW, Urbanek C, Groshong SD, Cosgrove GP, Brown KK, Schwarz
440 MI, Schwartz DA, Reynolds SD: The idiopathic pulmonary fibrosis honeycomb cyst contains
441 a mucociliary pseudostratified epithelium. *PLoS One* 2013, 8:e58658.

- 442 [34] Scotton CJ, Chambers RC: Molecular targets in pulmonary fibrosis: the myofibroblast in
443 focus. *Chest* 2007, 132:1311-21.
- 444 [35] Blackwell TS, Tager AM, Borok Z, Moore BB, Schwartz DA, Anstrom KJ, Bar-Joseph Z,
445 Bitterman P, Blackburn MR, Bradford W, Brown KK, Chapman HA, Collard HR, Cosgrove
446 GP, Deterding R, Doyle R, Flaherty KR, Garcia CK, Hagood JS, Henke CA, Herzog E,
447 Hogaboam CM, Horowitz JC, King TE, Jr., Loyd JE, Lawson WE, Marsh CB, Noble PW, Noth
448 I, Sheppard D, Olsson J, Ortiz LA, O'Riordan TG, Oury TD, Raghu G, Roman J, Sime PJ,
449 Sisson TH, Tschumperlin D, Violette SM, Weaver TE, Wells RG, White ES, Kaminski N,
450 Martinez FJ, Wynn TA, Thannickal VJ, Eu JP: Future directions in idiopathic pulmonary
451 fibrosis research. An NHLBI workshop report. *Am J Respir Crit Care Med* 2014, 189:214-22.
- 452 [36] Marchal-Somme J, Uzunhan Y, Marchand-Adam S, Valeyre D, Soumelis V, Crestani B,
453 Soler P: Cutting edge: nonproliferating mature immune cells form a novel type of organized
454 lymphoid structure in idiopathic pulmonary fibrosis. *J Immunol* 2006, 176:5735-9.
- 455 [37] Campbell DA, Poulter LW, Janossy G, du Bois RM: Immunohistological analysis of lung
456 tissue from patients with cryptogenic fibrosing alveolitis suggesting local expression of immune
457 hypersensitivity. *Thorax* 1985, 40:405-11.
- 458 [38] Idiopathic Pulmonary Fibrosis Clinical Research N, Raghu G, Anstrom KJ, King TE, Jr.,
459 Lasky JA, Martinez FJ: Prednisone, azathioprine, and N-acetylcysteine for pulmonary fibrosis.
460 *N Engl J Med* 2012, 366:1968-77.
- 461 [39] Zhang L, Wang Y, Wu G, Xiong W, Gu W, Wang CY: Macrophages: friend or foe in
462 idiopathic pulmonary fibrosis? *Respir Res* 2018, 19:170.
- 463 [40] Allden SJ, Ogger PP, Ghai P, McErlean P, Hewitt R, Toshner R, Walker SA, Saunders P,
464 Kingston S, Molyneaux PL, Maher TM, Lloyd CM, Byrne AJ: The Transferrin Receptor CD71
465 Delineates Functionally Distinct Airway Macrophage Subsets during Idiopathic Pulmonary
466 Fibrosis. *Am J Respir Crit Care Med* 2019, 200:209-19.

467 [41] Song E, Ouyang N, Horbelt M, Antus B, Wang M, Exton MS: Influence of alternatively
468 and classically activated macrophages on fibrogenic activities of human fibroblasts. *Cell*
469 *Immunol* 2000, 204:19-28.

470

471

472 **Figure legend**

473

474 **Figure 1. Examples of pathological scores on IPF tissue section**

475 H&E staining. (A) Mild patchy fibrosis (score=1) without honeycomb cysts formation
476 (score=0) or emphysema (score=0). (B) Severe patchy fibrosis (score=3) without honeycomb
477 cysts formation (score=0) or emphysema (score=0). (C) Mild patchy fibrosis (score=1) and
478 emphysema (score=1) without honeycomb cysts formation (score=0). (D) Severe patchy
479 fibrosis (score=3) and honeycomb (score=1) without emphysema (score=0). Scale bar indicates
480 2mm.

481

482 **Figure 2. Comparisons of microCT measures between regions with and without**
483 **honeycomb cysts formation in IPF samples.**

484 H&E staining. (A) Patchy fibrosis (score =2) without honeycomb cysts formation (score=0).
485 (B) Patchy fibrosis (score =2) with honeycomb cysts formation (score = 1). Arrow indicates
486 honeycomb region. The histological sections were matched with microCT images. (C and D)
487 The alveolar surface density and number of terminal bronchioles per ml lung volume on
488 microCT were decreased in honeycomb regions (n=12) compared to non-honeycomb regions
489 (n=47). * indicates $p<0.05$. (E) Three-dimensional rendering of the small airway tree (pink)
490 overlaid onto microCT images from the same stack as used in panel B (see also online
491 supplemental video 1). The small airway was connected with airspace in the honeycomb region
492 (orange).

493

494

495

496 **Figure 3. Comparisons of alveolar surface density and number of terminal bronchioles**
497 **between non-emphysematous regions with and without honeycomb cysts formation.**

498 (A) The alveolar surface density and (B) Number of terminal bronchioles were compared
499 between control, non-emphysematous IPF samples with and without honeycomb regions (n=36,
500 10, and 23). The absence of emphysema was determined based on the histological emphysema
501 score of 0. * indicates $p < 0.05$ compared to controls. † indicates $p < 0.05$ compared to non-
502 emphysematous IPF samples without honeycomb regions.

503

504

505 **Tables**

506

507 **Table1. Demographic data of subjects**

	Control (N=6)	IPF (N=10)
Age	58 ± 10	57 ± 5
Height (cm)	175 ± 6	173 ± 7
Weight (kg)	80 ± 15	73 ± 10
Sex	M : F = 6 : 0	M : F = 10 : 0
Smoking history	F : N = 2 : 4	F : N = 10 : 0
FEV ₁ (% predicted)	NA	61 ± 15
FVC (% predicted)	NA	59 ± 20
D _{LCO} (% predicted)	NA	28 ± 8

508 IPF = idiopathic pulmonary fibrosis. M : F = Male : Female. F : N = Former smoker : Never
509 smoker. FEV₁ = forced expiratory volume in one second, FVC= Forced vital capacity, D_{LCO}=
510 diffusing capacity for carbon monoxide.

511

512

513 **Table2. Comparisons of microCT and histological findings between control and IPF**

	Control	IPF
No. tissue cores	36	60
MicroCT		
Alveolar surface density (/mm)	15.5 ± 2.0	8.9 ± 3.6**
Tissue% (%)	28.4 ± 3.7	50.5 ± 14.2**
Lm (um)	360 ± 53	529 ± 298**
No. terminal bronchioles/ml lung	4.1 ± 1.6	1.8 ± 1.3**
Histology scoring		
Patchy fibrosis	NA	1.3 ± 1.0
Fibroblastic Foci	NA	0.8 ± 0.8
Honeycomb	NA	0.2 ± 0.5
CD68	0.7 ± 0.5	1.6 ± 0.6**
CD4	0.4 ± 0.6	1.6 ± 0.7**
CD8	1.1 ± 0.4	1.6 ± 0.6**
CD79a	0.1 ± 0.3	1.2 ± 0.8**
Lymphoid follicle	0 ± 0	0.8 ± 0.8**

514 Tissue%=total lung volume taken up by tissue, Lm =the mean linear intercept. All scores range

515 from 0 to 3. NA = not available. **<p<0.005.

516

517

518 **Table 3. Spearman correlation coefficients between microCT indices and pathological**
519 **scores in IPF samples**

	Alveolar surface density	Tissue%	Lm	No. terminal bronchioles
Major criteria for UIP				
Patchy fibrosis	-0.66**	0.69**	0.41**	-0.02
Fibroblastic foci	-0.52**	0.58**	0.39**	0.05
Honeycomb	-0.53**	0.38**	0.40**	-0.34**
Other scores				
Emphysema	0.01	-0.56**	0.19	-0.09
Inflammation	-0.25	0.31*	-0.03	0.09
Hyaline membrane	0.01	0.06	-0.13	0.00
Respiratory bronchiolitis	0.18	-0.17	-0.14	0.00

520 Tissue%=total lung volume taken up by tissue, Lm =the mean linear intercept.

521 *p<0.05, **<p<0.005.

522

523

524 **Table 4. Spearman correlation coefficients between microCT indices and scores of**
525 **infiltrated inflammatory immune cells in IPF samples**

	Alveolar surface density	Tissue%	Lm	No. terminal bronchioles
CD68	-0.20	0.49**	0.02	0.20
CD4	-0.11	0.30*	0.09	0.19
CD8	-0.17	0.41**	0.05	0.09
CD79a	-0.44**	0.53**	0.19	0.03
Lymphoid follicle	-0.41**	0.44**	0.14	-0.06

526 Tissue%=total lung volume taken up by tissue, Lm =the mean linear intercept.

527 *p<0.05, **<p<0.005.

528

Figure 1

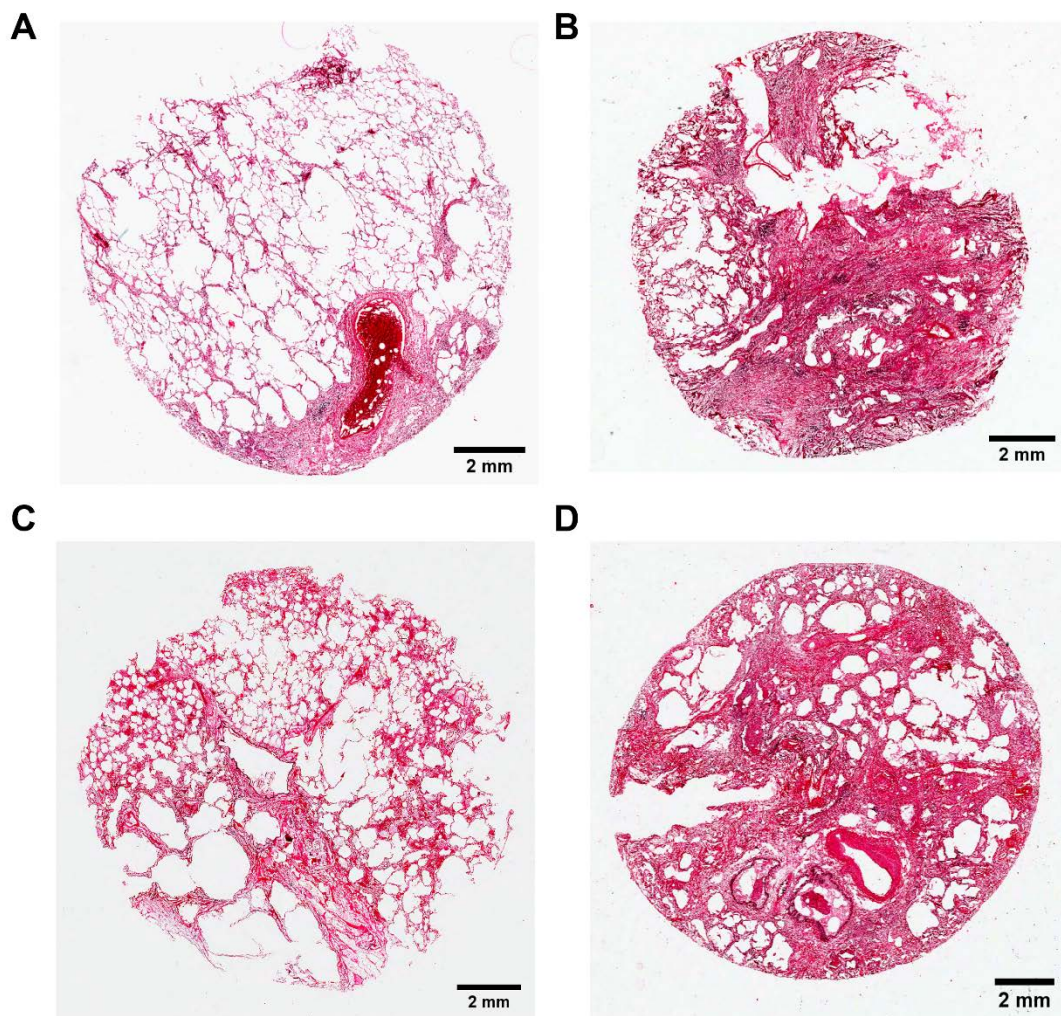


Figure 2

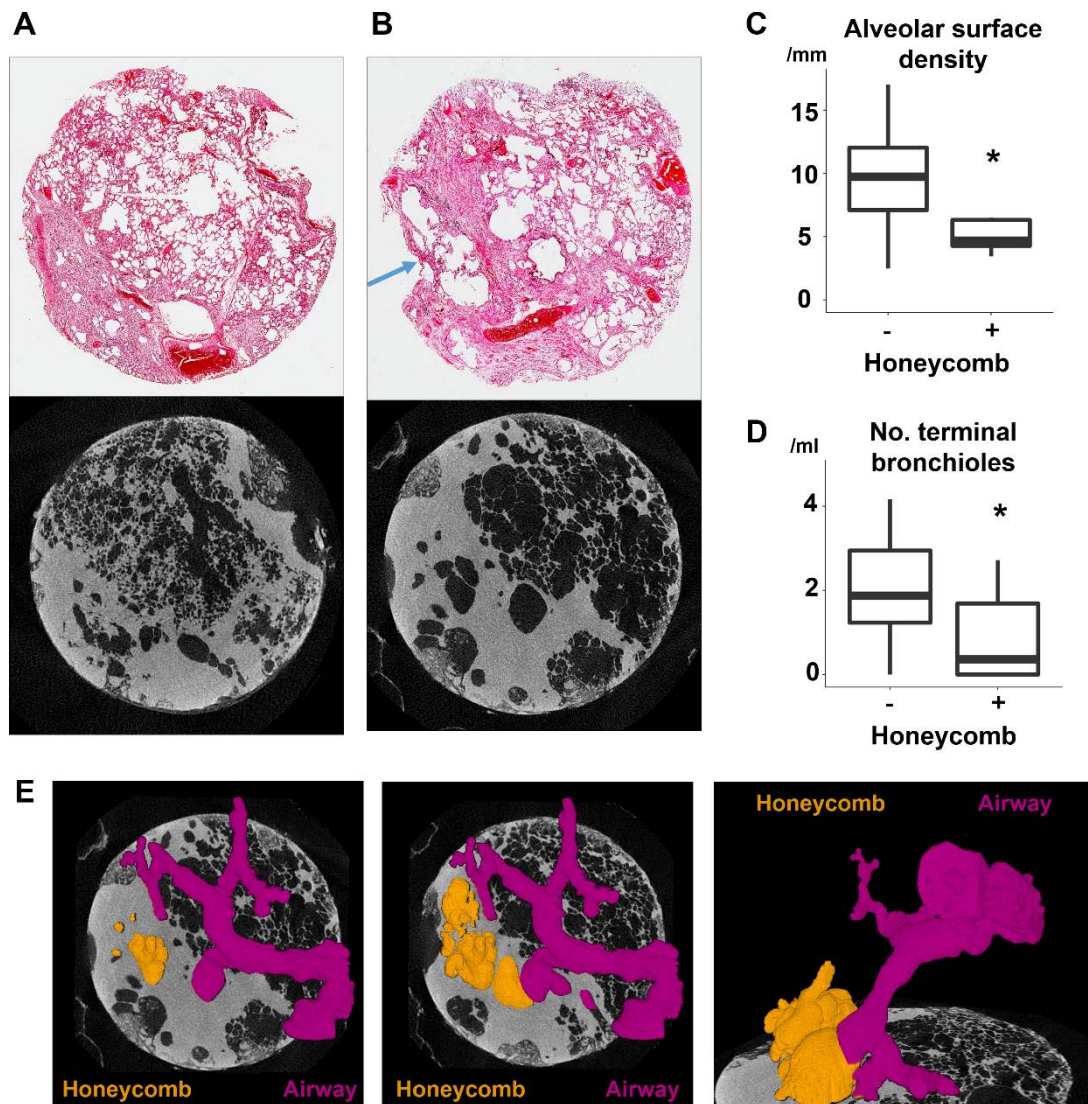


Figure 3

